

Miniaturised Flame Ionisation Detector for Explosion Protection in Civil Sewerage Networks

Jan Förster¹(✉), Winfred Kuipers², Christian Koch¹, Christian Lenz³,
Steffen Ziesche³, and Dominik Jurkow⁴

¹ Krohne Innovation GmbH, Ludwig-Krohne-Str. 5, 47058 Duisburg, Germany
j.foerster@krohne.com

² Krohne Messtechnik GmbH, Ludwig-Krohne-Str. 5,
47058 Duisburg, Germany

³ Fraunhofer Institut IKTS, Winterbergstr. 28, 01277 Dresden, Germany

⁴ VIA Electronics, Robert-Friese Str. 3, 07629 Hermsdorf, Germany

Abstract. This work presents a new approach to enhance the civil safety by monitoring the civil sewerage networks to prevent formation of explosive atmospheres and thus enabling early initialisation of counter measures. For this approach a new system with a miniaturised flame ionisation detector (FID) as embedded sensor has been developed. The micro FID embeds the fluidic components, the micro burner, the electrical structures for ignition and ion current measurement, and resistive temperature measurement elements in one monolithic ceramic component. Characterisation of the micro FID revealed good sensor performance with high sensitivity and reduced gas consumption compared to conventional FIDs. Thus, this micro FID is an excellent choice for an embedded sensor in the context of monitoring the civil sewerage.

Keywords: Monitoring of civil infrastructure · Civil safety · Embedded sensor · Flame ionisation detector · Ceramic multilayer technology

1 Introduction

Civil sewerage networks provide a higher explosion risk for the general public than commonly assumed. Accidentally spilled fuels, traffic accidents, or even wilfully inserted flammable fluids might easily lead to an explosive atmosphere in the sewerage networks. In addition, slow running or residential waste water can form atmospheres with a high concentration of fermentation gases, which also leads to an explosive atmosphere in the sewerage networks. Explosions in the sewerage networks are especially dangerous because they normally result in massive destruction of the infrastructure. Thus, they have a high potential risk of injuring the general public. Explosions in the sewerage networks due to flammable fluids as well as due to fermentation gases have already repeatedly led to massive infrastructure damage and injuries of affected persons [1, 2]. Therefore, it is necessary to minimise the explosion risk in the sewerage networks.

A minimisation of the explosion risk can only be achieved by continuous monitoring of the atmosphere in the sewerage, which allows detecting the potential formation of an explosive atmosphere at a very early stage. Thus, countermeasures can be initiated in time to prevent the formation of explosive atmospheres. Estimations of the potential explosion risk show that risk mitigation by continuous monitoring can reduce the explosion risk for critical locations from a high risk for the public to moderate or small risk. Unfortunately, devices for continuous monitoring of the sewerage do not exist yet. Nowadays, the atmosphere of the sewerage is only measured intermittently during maintenance work. Therefore, this work aims to build a system with embedded sensing which allows the continuous monitoring of the civil sewerage networks.

In order to be capable of detecting a potential formation of an explosive atmosphere at an early stage, the system needs a very sensitive sensing element. For this sensing element a variety of measurement principles exist (e.g. IR absorption sensor, catalytic heat tone sensor, electrochemical sensor, flame ionisation detector). Most of these measurement principles do not provide a sufficient sensitivity or selectivity to allow a reliable early detection of the formation of an explosive atmosphere. In addition, many of these measurement principles are not applicable to the harsh environmental conditions of the sewerage. However, the flame ionisation detector (FID) has a very high sensitivity and selectivity towards hydrocarbons and is therefore an adequate measurement principle in this context. Furthermore, the FID is quite insensitive to the environmental conditions in the sewerage network. These properties make the FID the ideal measurement principle for a system with embedded sensing to monitor the sewerage.

2 FID Theory and System Overview

In order to better understand the functionality of the system a short introduction of the working principle of an FID is given before the embedded sensing is explained.

2.1 Working Principle of an FID

The working principle of an FID is based on the ionisation of organic material in a hydrogen flame and the detection of the resulting ion current in an electric field [3]. Figure 1 shows a schematic drawing of a conventional FID. In an FID, hydrogen and air are inserted by nozzles into a burning chamber where the hydrogen is ignited. Normally, FIDs have a very high gas consumption of at least 30 ml/min hydrogen and 300 ml/min air [4]. Sample gas containing organic material to be analysed is added to the hydrogen. The organic material is ionised in the hydrogen flame. An electric field applied to the hydrogen flame extracts these ions. As a result, these ions generate a small current which is direct proportional to the amount of hydrocarbons in the organic material.

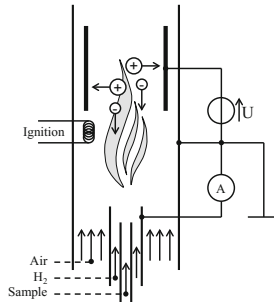
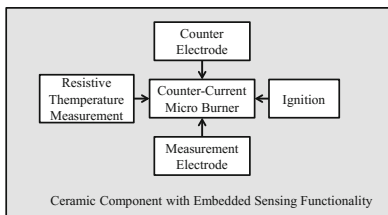


Fig. 1. Schematic drawing of a conventional FID

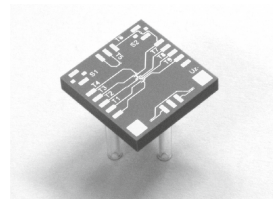
2.2 The Micro FID as Embedded Sensor

The overall system consists of the embedded sensing device and some peripherals for controlling. The embedded sensing device of the system consists of the FID with all its necessary elements. The aforementioned high gas consumption of conventional FIDs is not applicable to the context of monitoring the sewerage where reduced gas consumption is essential to allow long intervals between maintenance of the system. Here, miniaturised FIDs might offer adequate solutions with reduced gas consumption and appropriate sensor properties [5–7]. In addition, miniaturised FIDs allow the use of pure oxygen as a combustion gas instead of air, which leads to a further reduction of gas consumption [7]. However, these miniaturised FIDs suffer from reduced long term stability due to the non-monolithic integration in silicon-based microsystems. Therefore, our novel approach embeds the full FID system with its electrical and fluidic functionality in a monolithic ceramic component. This approach does not only combine the reduced gas consumption and good sensor performance of miniaturised FIDs and the excellent long term stability of a monolithic ceramic body, but also adds the benefit of cost-effective batch fabrication [8].

Figure 2a shows a schematic drawing of the micro FID. As shown, this ceramic component embeds electrical and fluidic components in a monolithic ceramic body. It consists of a micro burner in counter-current configuration for the hydrogen flame,



(a)



(b)

Fig. 2. Schematic drawing of the micro FID (a) and a photograph of the constructed micro FID (b)

ignition elements to start the hydrogen flame, counter and measurement electrodes to extract the generated ions, and several resistive thermometers to monitor the burning process. In order to analyse the effect of the micro burner on the sensor properties different nozzle sizes have been implemented.

Figure 2b shows a photograph of the micro FID with its electrical connections above and its fluidic interfaces underneath. The whole micro FID with all necessary internal components realised has outer dimensions of just $1.5\text{ cm} \times 1.5\text{ cm} \times 0.25\text{ cm}$. It was manufactured in a monolithic low temperature cofired ceramic (LTCC) body using multilayer technology [8]. This technology allows the 3D-integration of electrical and fluidic elements by stacking and laminating of multiple structured LTCC green tapes followed by a co-firing process.

As mentioned before, some additional peripherals complete the system. These peripherals consist of components for the control of the gas flows, components for the power supply, and components to acquire the data of the embedded sensing device.

3 Characterisation of the Micro FID

The micro FID is the most important part of the described system. Thus, characterisation of its properties to analyse its functionality is crucial. Therefore, comprehensive measurements to determine gas consumption, sensitivity, noise, and detection limits of the micro FID have been performed with a fundamental measurement setup. This measurement setup can be transformed into a fully functional demonstration device by just a few further developments.

3.1 Measurement Setup

As shown in Fig. 3 the laboratory measurement setup consists of components to control the gas flows, the sample gas composition, and the electrical supplies. In order to achieve precise gas flows at low gas flow rates flow controllers are used to set the gas flows of the combustion gases. In addition, gas cylinders with nitrogen and a mixture of 1% methane (CH_4) in nitrogen are installed to provide sample gases. With the help of mass flow controllers and valves these two gases can be combined in any composition which enables detailed sensitivity measurements with this setup. The already existing peripheral components of the system for the control of the ignition, the generation of the

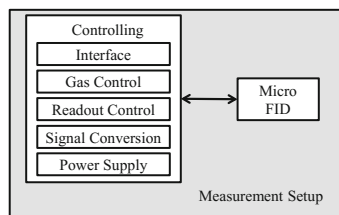


Fig. 3. Schematic drawing of the measurement setup

polarisation voltage and the ion current measurement are used in this measurement setup. Thus, just the timing control of the measurements and the handling of the measurement data have been realized in a Matlab™ programme on the measurement PC.

3.2 Determination of Minimum Gas Consumption

The first step of the characterisation was to determine the minimum gas consumption. As the hydrogen flame inside the micro FID cannot be visually inspected, the easiest way to monitor whether the flame is burning or not is measuring the surface temperature. If the hydrogen flame is burning, the surface temperature rises significantly within a few seconds.

Figure 4 shows the spatial distribution of the temperature at the surface of the micro FID for gas flows of 24 ml/min hydrogen and 12 ml/min oxygen. For a better orientation, the micro burner inside the micro FID is illustrated by a dotted line. As can be seen in the thermal image in Fig. 4, the hottest point of the surface is in the centre. At this point, the two combustion gases coming out of the nozzles mix and form the hydrogen flame. Furthermore, Fig. 4 shows that the temperature distribution follows the geometry of the micro burner because the temperature at the outlets is higher than the temperature at the nozzle inlets. Generally, from Fig. 4 it can be said, that the surface temperature decreases with rising distance from the center. Therefore, for the determination of the minimum gas flows, only the temperature at the centre of the surface has been taken into account.

Figure 5 illustrates the measured surface temperature at different gas flow rates of hydrogen and oxygen (always half of the hydrogen flow) for four different sizes of the micro burner nozzles. To enhance the readability of the graph, only results for a burning hydrogen flame are plotted in Fig. 5. As can be seen in that figure, the surface temperature rises with increasing gas flow rates. Furthermore, it can be seen that the micro burner with the biggest nozzle size needs at least gas flows of about 16 ml/min hydrogen and 8 ml/min oxygen to keep the hydrogen flame stable. At lower gas flow rates the hydrogen flame extinguishes. For smaller nozzle sizes the gas flows can be further reduced. The micro burner with half the nozzle size needs at least only approximately 10 ml/min hydrogen and 5 ml/min oxygen to keep the hydrogen flame

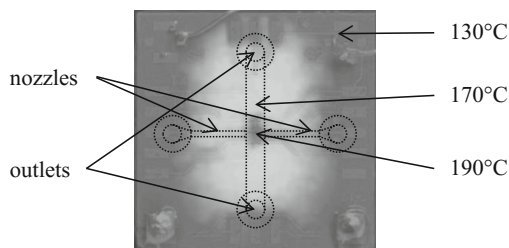


Fig. 4. Overlap of photograph of the micro FID surface and thermal image in false colour representation showing the spatial distribution of the surface temperature

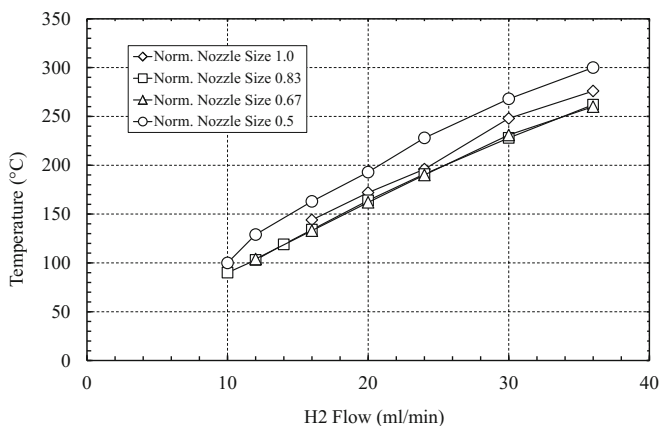


Fig. 5. Surface temperature at the centre of the micro FID vs. hydrogen gas flow for four different nozzle sizes and stoichiometric oxygen gas flow

alive. On the one hand, these minimum gas flow rates are below the necessary gas consumption of a conventional FID. On the other hand, even lower minimum gas flow rates for other micro FIDs have been reported in literature [9]. However, in the context of our application these gas flow rates were small enough to continue with the characterisation.

3.3 Sensitivity

The first step for the characterisation of the sensitivity of the micro FID is the determination of an adequate operating point, i.e., finding the best relation between polarisation voltage and current. Therefore, the gas flows of hydrogen and oxygen as well as the flow of the sample gas are set to a constant value while the polarisation voltage is swept from -100 V to $+100$ V. The result of such a measurement is shown in Fig. 6a. For that measurement the gas flows for hydrogen and oxygen have been set to 20 ml/min and 10 ml/min respectively. The sample gas composition consisted of 9000 ppm methane in nitrogen and its flow was 10 ml/min. As can be seen in Fig. 6a, the current as a function of the polarisation voltage is almost symmetric. For low polarisation voltages the current strongly increases with rising polarisation voltage until it saturates for a polarisation voltages of about 20 V. Therefore, the operating point of the micro FID is defined at a polarisation voltage of 20 V. All following measurements for the characterisation of the sensitivity have been performed at this operating point.

To determine the sensitivity of the micro FID, the gas flows of hydrogen and oxygen are set to a constant value again and the polarisation voltage is set to the operating point. The flow of the sample gas is also set to a constant value, whereas its composition is varied between a content of 1000 ppm methane in nitrogen and 9000 ppm methane in nitrogen. The result for such a measurement with a hydrogen flow of 20 ml/min, an oxygen flow of 10 ml/min, and a sample flow of 10 ml/min is

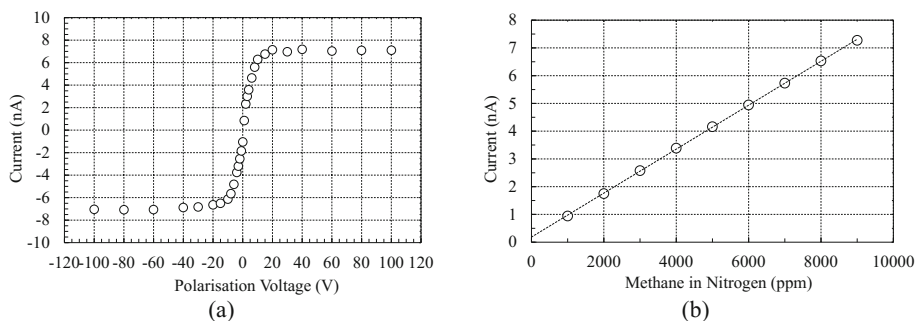


Fig. 6. Measured current for a constant sample gas composition as a function of the applied polarisation voltage (a) and measured current for a constant polarisation voltage as a function of the sample gas composition (b)

shown in Fig. 6b. As can be seen in this figure, the current linearly increases with growing methane content in the sample gas. This behaviour is as expected from an FID.

The sensitivity of the micro FID can be extracted from Fig. 6b. Its value corresponds to the slope of the current as a function of the sample gas composition. Here, the relative sensitivity is approximately 0.79 pA per 1 ppm methane in nitrogen. The relative sensitivity is a direct measure of how much current is to be expected at a certain content of organic material in the analysed sample. In the context of monitoring the civil sewerage this parameter is of high importance because it determines the possible detection resolution of the embedded sensing of the system.

However, the relative sensitivity does not give any information on how effective the FID works. To determine the effectiveness of the FID the absolute amount of organic material in the analysed sample must be taken into account. Thus, this kind of sensitivity shows how much charge carriers of an organic sample are ionised. As this value corresponds to the absolute amount of organic material, it is referred to as absolute sensitivity. Even if this value is not as crucial in the context of monitoring the civil sewerage as the relative sensitivity, it is the main parameter FIDs are compared by. For the given scenario in Fig. 6b the absolute sensitivity is approximately 8.86 mC/gC, which is lower than the values of up to 15 mC/gC reported for conventional or micro FIDs [3, 10].

Both, the relative sensitivity value and the absolute sensitivity value are valid for one specific set of gas flows only. If any of the gas flows change, the sensitivity value will change too. Therefore, the relative and the absolute sensitivity of the micro FID have been determined for multiple sample gas flows as well as for several combustion gas flows. The sample flow has been varied from 1 ml/min to 16 ml/min. The hydrogen flow has been set to 12 ml/min, 16 ml/min, 20 ml/min, and 24 ml/min and the oxygen flow was always set to half of the hydrogen flow.

The results for constant hydrogen and oxygen flows of 24 ml/min and 12 ml/min respectively are shown in Fig. 7. As can be seen from Fig. 7a, the relative sensitivity increases with growing sample flow until it levels out or even decreases again with further growing sample flows. The sample flow which corresponds to the highest

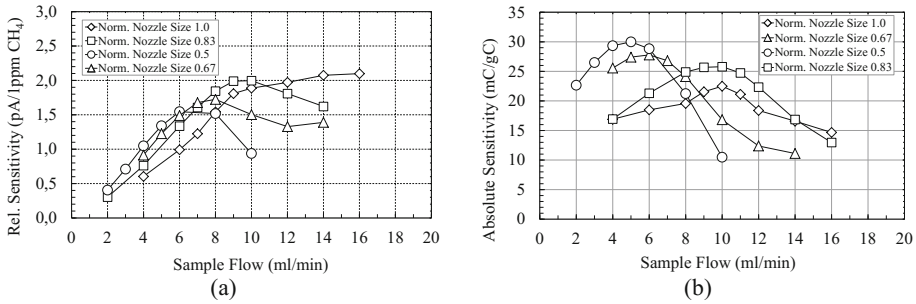


Fig. 7. Relative sensitivity (a) and absolute sensitivity (b) as a function of the sample flow for a constant hydrogen and oxygen flow of 24 ml/min and 12 ml/min respectively

relative sensitivity of a micro FID shifts from 6 ml/min to 14 ml/min with increasing FID nozzle size. In addition, a higher maximum value can be reached with increasing nozzle size. Figure 7b shows that the absolute sensitivity of the micro FIDs first increases with growing sample gas flows and then decreases again with further growing sample gas flows. Just like for the relative sensitivity, the maximum values of the absolute sensitivity shift to higher sample flow rates with increasing nozzle size. In contrast to the relative sensitivity, the maximum value of the absolute sensitivity is accomplished by the micro FID with the smallest nozzle. The absolute sensitivity of approximately 29.9 mC/gC is twice as high as the values reported in literature [3, 10]. This indicates an outstandingly good effectiveness of the developed micro FID.

The maximum values of the relative and the absolute sensitivity for the other sets of hydrogen and oxygen flows are summarised in Tables 1 and 2. The sample gas flows for the results shown in these tables correspond to the sample gas flows for the maximum values in Fig. 7a and b. The results from these two tables show that both, the relative and the absolute sensitivity, decrease with reduced hydrogen and oxygen flows. However, the overall dependency of the relative and absolute sensitivity on the sample flow as described before still occurs at reduced hydrogen and oxygen flows. Thus, a trade-off between gas consumption and sensitivity has to be found to match the requirements for the embedded sensor in the context of monitoring the civil sewerage.

Table 1. Maximum values of the relative sensitivity for given hydrogen and oxygen flows

Hydrogen and oxygen Flow (ml/min)	Relative sensitivity (pA/1 ppm methane)			
	1.0	0.83	0.67	0.5
Norm. nozzle size	1.0	0.83	0.67	0.5
12/06	–	–	–	0.43
16/08	–	1.06	0.91	0.76
20/10	1.49	1.54	1.34	1.13
24/12	2.10	2.00	1.72	1.55

Table 2. Maximum values of the absolute sensitivity for given hydrogen and oxygen flows

Hydrogen and oxygen flow (ml/min)	Absolute sensitivity (mC/gC)			
	1.0	0.83	0.67	0.5
Norm. nozzle size	1.0	0.83	0.67	0.5
12/06	–	–	–	10.7
16/08	–	15.4	16.2	16.8
20/10	16.4	20.9	22.2	23.5
24/12	22.4	25.7	27.7	29.9

3.4 Noise, Leakage Current and Detection Limit

In theory, the embedded sensor could yield a very low detection limit with the reported values of the relative sensitivity. The detection limit represents the smallest concentration of hydrocarbon in the sample gas which can be detected reliably. However, the detection limit is restricted by the noise of the micro FID [8].

In general, the noise of a micro FID originates in fluctuations of the hydrogen flame as well as in a leakage current [9]. If there is a leakage current present, its noise will contribute to the overall noise of the micro FID. The higher the leakage current is the more noise it will contribute to the overall noise. Therefore, measurements to determine leakage current and noise were of high interest.

Figure 6b shows that the dotted line representing the relative sensitivity does not meet the point of origin but has a small offset. This offset is due to leakage current, i.e. there is always a small current present in the micro FID even if there is no organic material in the sample. Thus, there is leakage current present in the micro FID which might contribute to the overall noise.

In order to determine the leakage current of the micro FIDs, the flows of hydrogen and oxygen are set to specific values while the sample composition is constantly set to pure nitrogen. The polarisation voltage is then swept from -100 V to $+100$ V. The result of such a measurement for hydrogen and oxygen flows of 20 ml/min and 10 ml/min respectively is shown in Fig. 8a. The graph shows a clear ohmic behaviour, which corresponds to a system resistance of approximately 24 G Ω .

The conductance of the ceramic material changes with temperature [8]. Therefore, the leakage current has been measured at several combustion gas flows to observe the influence of the combustion temperature on the insulation resistance. The results of these measurements are shown in Fig. 8b. The graph shows two different temperature regimes. For temperatures above 170 °C the insulation resistance decreases with rising temperature. This behaviour is in accordance to the physical understanding of an insulator. For temperatures less than 170 °C the insulation resistance decreases with falling temperature and even drops by several orders of magnitudes at a temperature around 100 °C. This behaviour is quite in contrast to the physical understanding of an insulator. However, it can be explained by the function of an FID. The product of the combustion of hydrogen and air is water vapour. This water vapour has a high vapour pressure. Thus, it starts to condense at temperatures just below 100 °C. As the hottest point of the micro FID is just above 100 °C, several parts of the micro FID are cooler

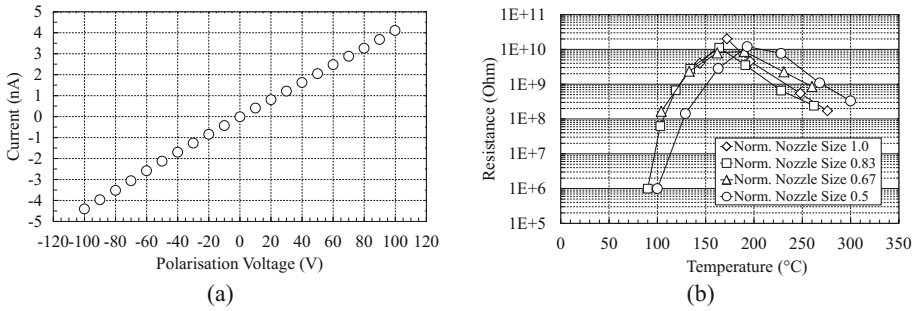


Fig. 8. Leakage current as a function of the polarisation voltage for hydrogen and oxygen flows of 20 ml/min and 10 ml/min respectively (a) and derived isolation resistance of the micro FIDs as a function of the surface temperature (b)

than 100 °C and thus, condensation of the water vapour occurs. The condensation film between the polarisation electrodes reduces the insulation resistance. Not only causes the condensation a high leakage current but it might also lead to fluidic disturbances. As a consequence, to obtain a working micro FID with low gas consumption measures against the condensation are obligatory.

As the operation of the micro FID with noticeable condensation effects does not represent realistic operating conditions at all, only measurements without any noticeable condensation effects are taken into account for the noise estimation. The noise was estimated using the standard deviation σ . It is defined as $\pm 3\sigma$ [9]. Therefore, the standard deviation of the signal during time periods of 100 s was calculated. As the signal to noise ratio is most crucial at very low signal levels, the noise estimations have been performed without any methane content in the sample gas. The results are shown in Fig. 9a. This graph shows that the noise increases from a few picoamperes to values above 30 pA with increasing hydrogen flow. As the temperature and thus the leakage current also rises with increasing hydrogen flow, it is most probable that there is a dependency of the noise on the leakage current. This dependency is shown in Fig. 9b. Here, it can be seen, that the noise increases with increasing leakage current. As the

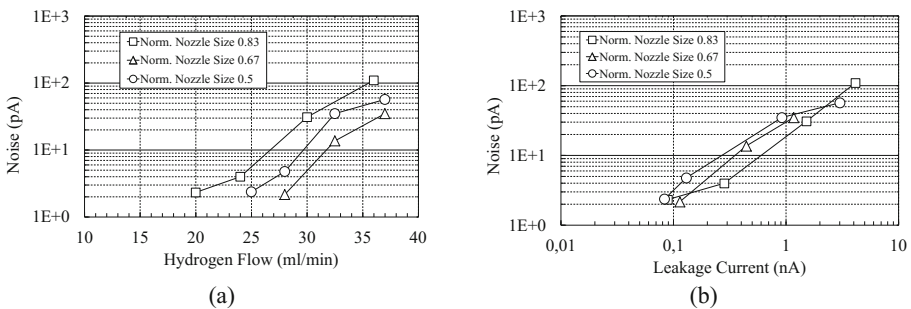


Fig. 9. Noise ($\pm 3\sigma$) of three different nozzle sizes as a function of the hydrogen flow (a) and as a function of the leakage current (b)

curves for different nozzle sizes overlap quite well, the noise presumably depends most strongly on the leakage current. Thus, reducing the leakage current by additional guard electrode structures should lead to a noticeable noise minimisation.

With these estimated noise values and the measured relative sensitivity values the detection limit of the micro FID can be calculated. It is defined as two times the noise divided by the relative sensitivity [9]. For the smallest noise value of 2.2 pA at an hydrogen flow of 20 ml/min and the corresponding relative sensitivity value of 1.73 pA/ppm the detection limit of the micro FID is approximately 2.5 ppm, i.e., a methane concentration of 2.5 ppm in the sample gas can be detected by our embedded sensor. For the lowest noise values of the micro FIDs with the other nozzle sizes comparable detection limits between 3 ppm and 4 ppm have been achieved.

In the context of monitoring the sewerage system these detection limits are more than adequate. Furthermore, the noise of our micro FID and its detection limit are in good accordance to the values of other micro FIDs reported in literature [9]. However, these values are not as good as the values of conventional FIDs [3, 4, 9].

4 Conclusion

A novel approach to enhance the civil safety by monitoring the sewerage networks for formation of explosive atmospheres with the help of a system using a miniaturised FID as an embedded sensor was presented. The micro FID was successfully produced using LTCC ceramic multilayer technology. The characterisation of the micro FID revealed a good overall performance. The gas consumption could be reduced to a hydrogen flow of 12 ml/min and an oxygen flow of 6 ml/min which is less than half of the hydrogen flow in conventional FIDs. Further reduction of the gas consumption might be achieved by improving the size of the ceramic body as well as by pre-heating the micro FID. The measured absolute sensitivity of 29.9 mC/gC testifies an excellent effectiveness of the micro FID. Thus, it can be used to detect small quantities of organic material in the sample gas. However, the noise level of several picoamperes limits the detection capability of the micro FID to approximately 2.5 ppm in the best case. Therefore, further improvement must deal with reducing the noise by introducing a guard electrode structure and thus minimising the leakage current.

Acknowledgments. This work is part of the project “FIDEX – Autonomer Mikroflammenionisations-detektor für den Explosionsschutz in zivilen Kanalisationsnetzen” and is financially supported by the German *Bundesministerium für Bildung und Forschung BMBF* (#13N13271).

References

1. Flammeninferno nach Explosion von Bahn-Zisternenwagen. *Neue Züricher Zeitung* (2009)
2. Explosion in der Kanalisation. *Stuttgarter Zeitung* (2016)
3. Hill, H.H., McMinn, D.G.: Detectors for capillary chromatography. *J. Chem. Anal.*, 7–21 (1992)

4. Amirav, A., Tzanani, N.: Electrolyzer-powered flame ionization detector. *Anal. Chem.* **69**, 1248–1255 (1997)
5. Zimmermann, S., Wischhusen, S., Müller, J.: Micro flame ionization detector and micro flame spectrometer. *J. Sens. Actuators B* **63**, 159–166 (2000)
6. Kuipers, W.J., Müller, J.: A planar micro-flame ionization detector with an integrated guard electrode. *J. Micromech. Microeng.* **18** (2008)
7. Kuipers, J., Müller, J.: Characterization of a microelectromechanical systems-based counter-current flame ionization detector. *J. Chromatogr. A* **1218**, 1891–1898 (2011)
8. Lenz, C., Neubert, H., Ziesche, S., Förster, J., Koch, C., Kuipers, W., Deilmann, M., Jurkow, D.: Development and characterization of a miniaturized flame ionization detector in ceramic multilayer technology for field applications. In: *Proceedings of Eurosensors* (2016)
9. Kuipers, W.J.: *Design, Fabrication and Characterization of a MEMS-Based Counter-Current Flame Ionization Detector*. Doktor Hut Verlag, München (2011)
10. Grob, R.L.: *Modern practice of gas chromatography*, 3rd edn. Wiley, New York (1995)